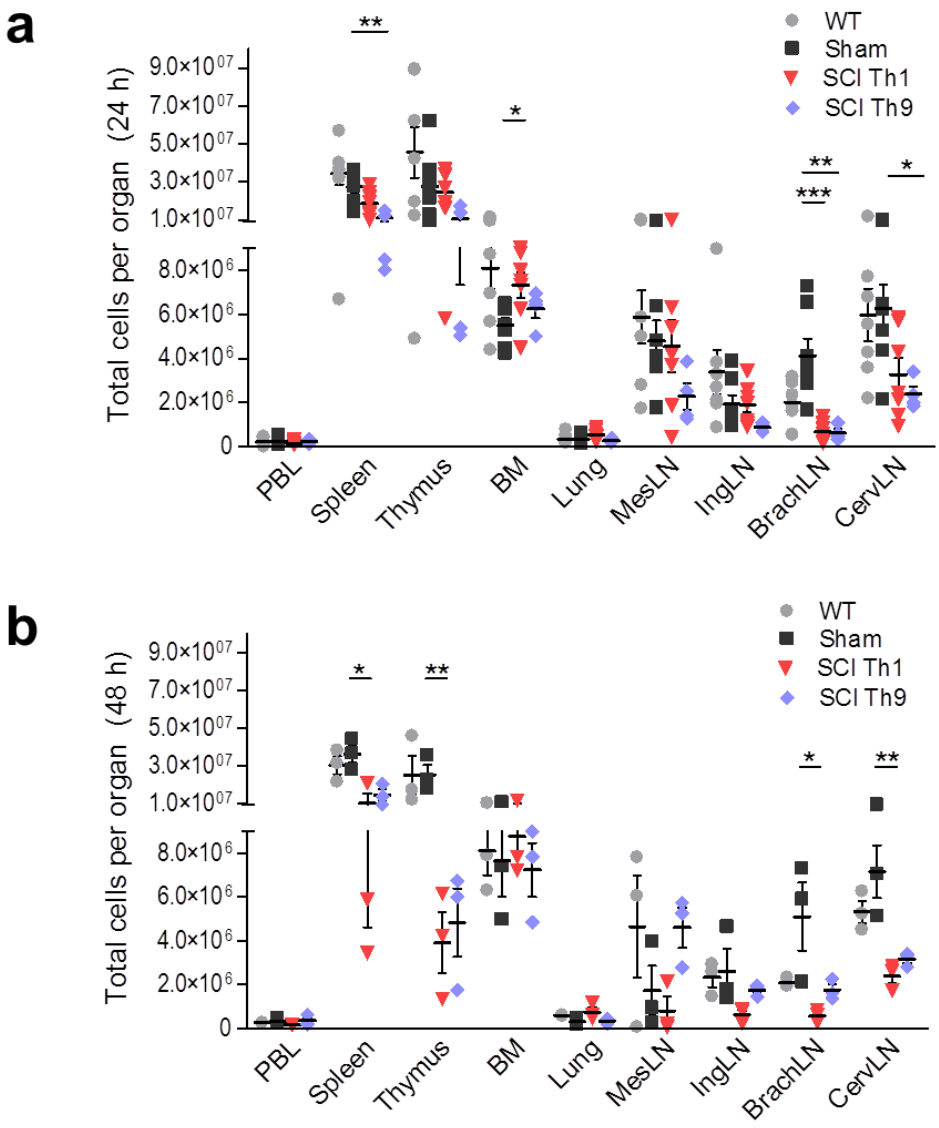

Supplementary Figure 1

Progressive reduction of organ cellularity after SCI.

The SCI-induced reduction in organ size was detectable already after 24 hours (**a**) and progresses continuously to 48 hours (**b**). Already at these early time points, cell loss is related to the level of SCI. Data are mean ± SEM, n=3 animals per group. * $p<0.05$; ** $p<0.01$; 1-way ANOVA with Tukey's multiple comparison test.

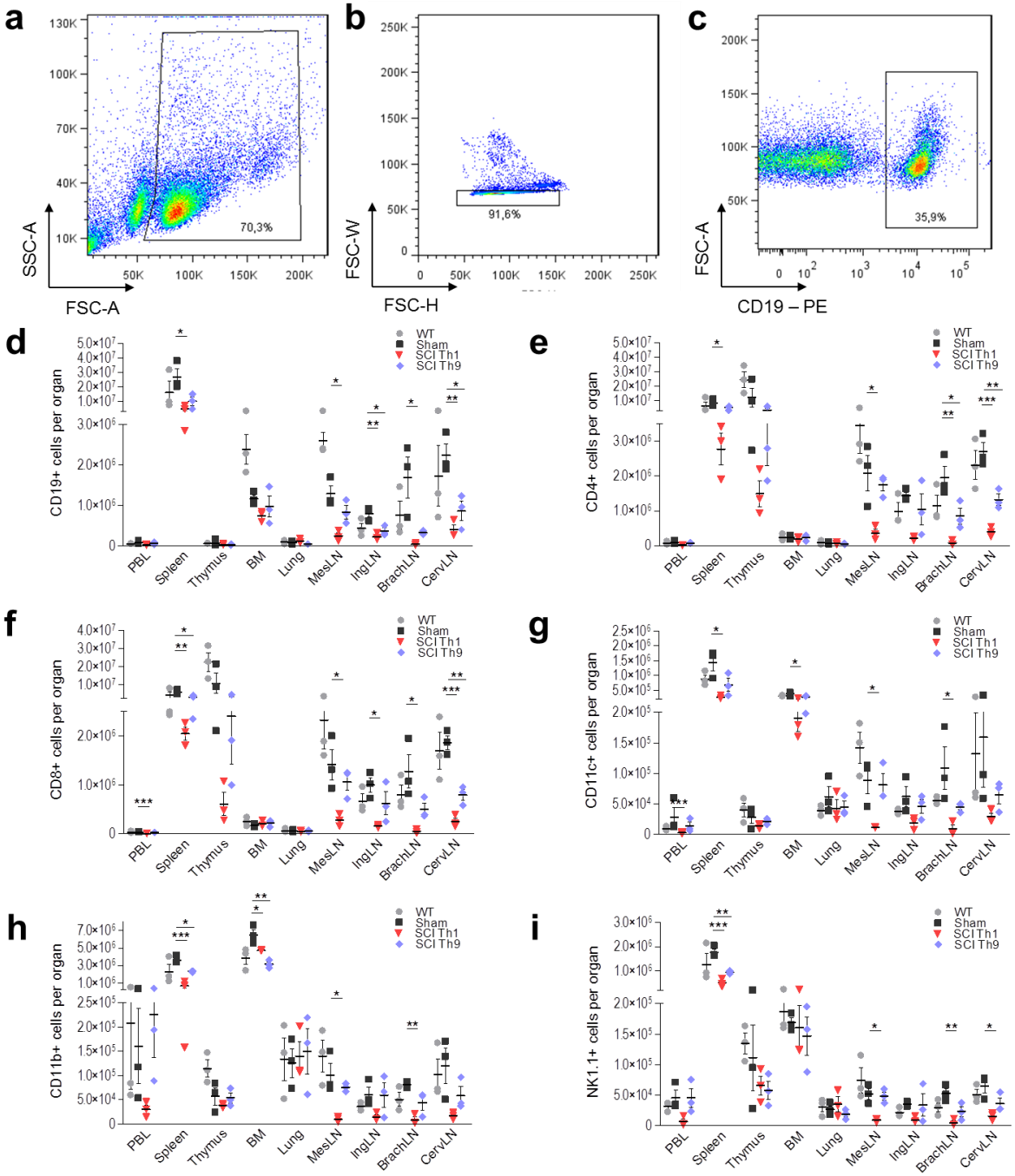

Supplementary Figure 2

SCI-induced cell depletion affects all analyzed types of immune cells.

FACS gating strategy exemplarily shown for $CD19^+$ B cells (**a**, leukocytes; **b**, single cells; **c**, $CD19^+$ cells). The profound cell loss affected all major immune cell populations including $CD19^+$ B cells (**d**), $CD4^+$ T cells (**e**), $CD8^+$ T cells (**f**), $CD11c^+$ dendritic cells (**g**), $CD11b^+$ monocytes (**h**), and $NK1.1^+$ NK cells (**i**). Data are mean ± SEM, n=3-5 animals per group. * p<0.05; ** p<0.01; *** p<0.001, 1-way ANOVA with Tukey's multiple comparison test.

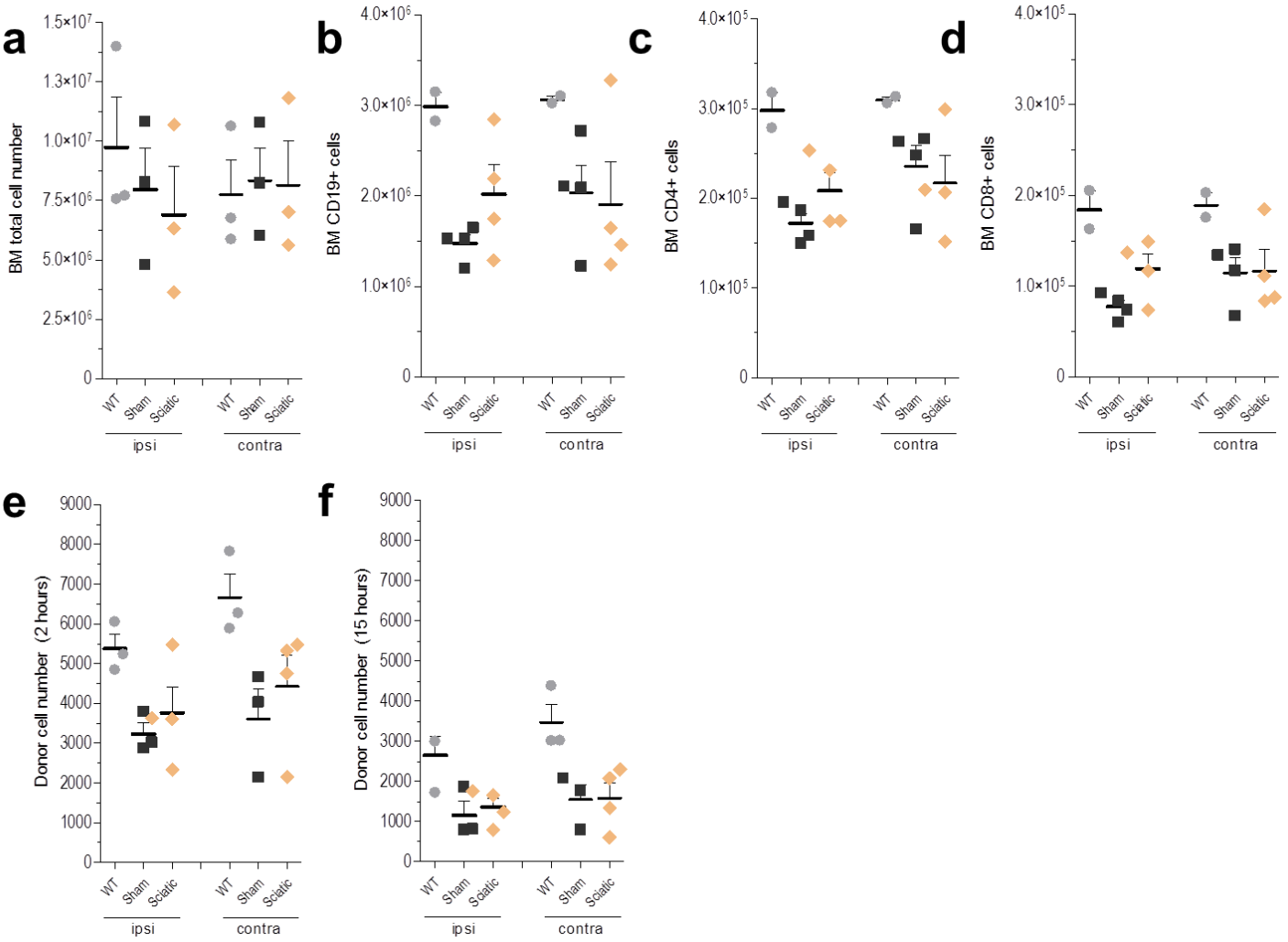

Supplementary Figure 3

Sciatic nerve lesion has no effect on immune cell composition of the innervated bone marrow.

(**a**) Deafferentiation of the tibial bone marrow by right sciatic nerve injury (compared to sham) did not change the total number of bone marrow cells. (**b-d**) Right sciatic nerve lesion did not change the number and frequency of $CD19^+$ (**b**), $CD4^+$ (**c**), $CD8^+$ (**d**), $Gr\text{-}1^+$, $NK1.1^+$, $CD11c^+$, and $CD11b^+$ cells (not shown) in the ipsi- and contralateral bone marrow. (**e-f**) Homing of donor splenocytes for 2 hours (**e**) as well as redistribution for 15 hours (**f**) to the bone marrow was equal in mice with right sciatic nerve lesion and sham-operated animals. Data are mean ± SEM, n=6-9 animals per group. * $p<0.05$; 1-way ANOVA with Tukey's multiple comparison test.

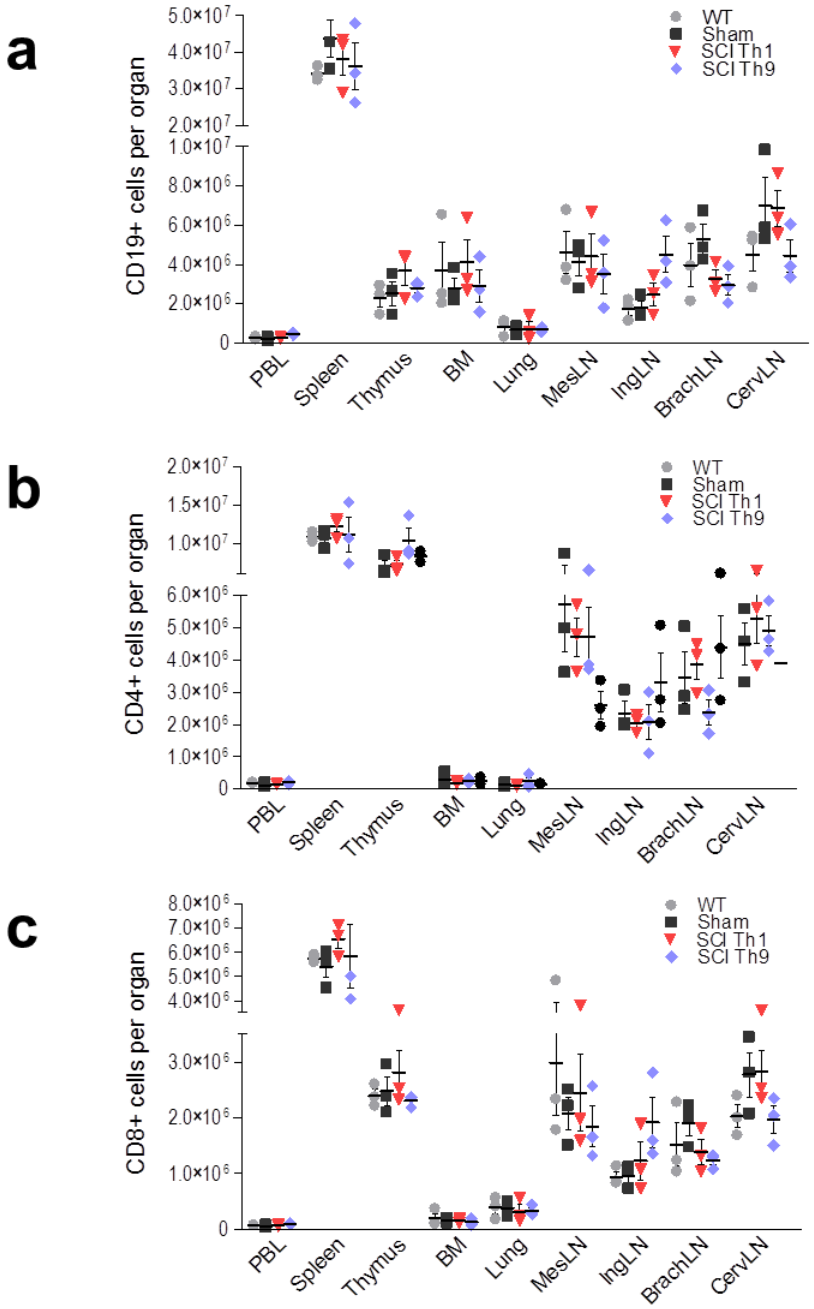

Supplementary Figure 4

Adrenalectomy reversed the SCI-induced cell depletion in all analyzed types of immune cells.

Adrenalectomy prevented the loss of all examined cell populations 72 hours after SCI. In particular, the number of $CD19^+$ (**a**), $CD4^+$ (**b**), $CD8^+$ (**c**), $CD11c^+$ and $CD11b^+$ cells (not shown) were unchanged after SCI. Data are mean ± SEM, n=3 animals per group. * $p<0.05$; ** $p<0.01$; *** $p<0.001$, 1-way ANOVA with Tukey's multiple comparison test.

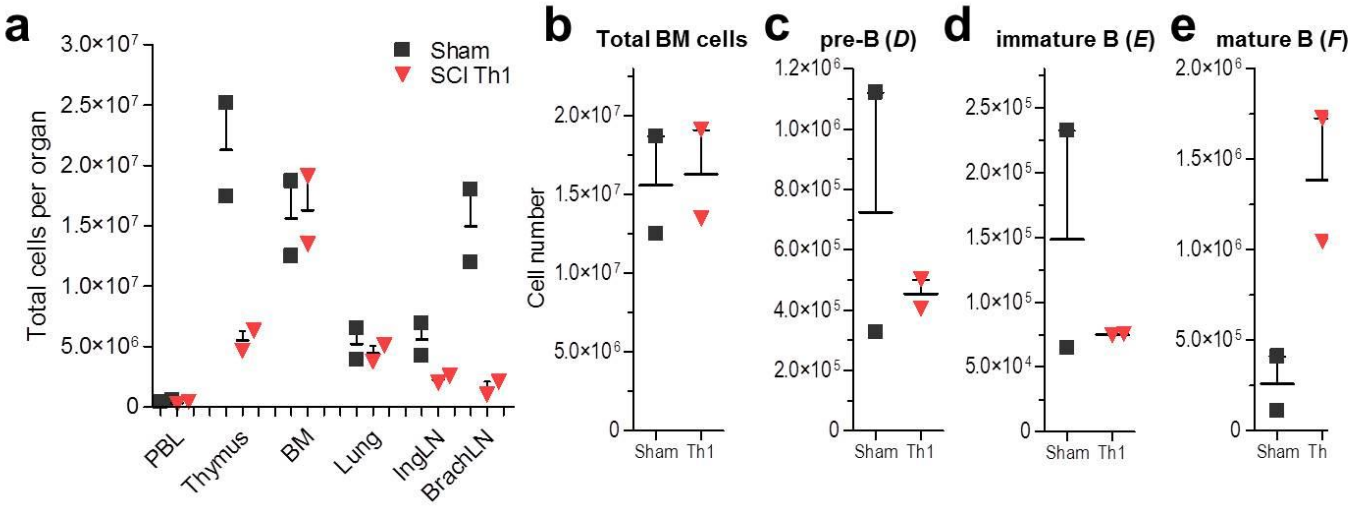

Supplementary Figure 5

Splenectomy did not reverse SCI-induced immune cell depletion.

In contrast to surgical removal of the adrenals, removal of the spleen which is similarly innervated by sympathetic fibers via the splanchnic nerve, could not re-establish the SCI-induced cell death in thymus and lymph nodes (**a**) and did not change the characteristic SCI-induced pattern of B cell populations in the bone marrow (**b-e**) with massive enrichment of mature B cells (**e**).

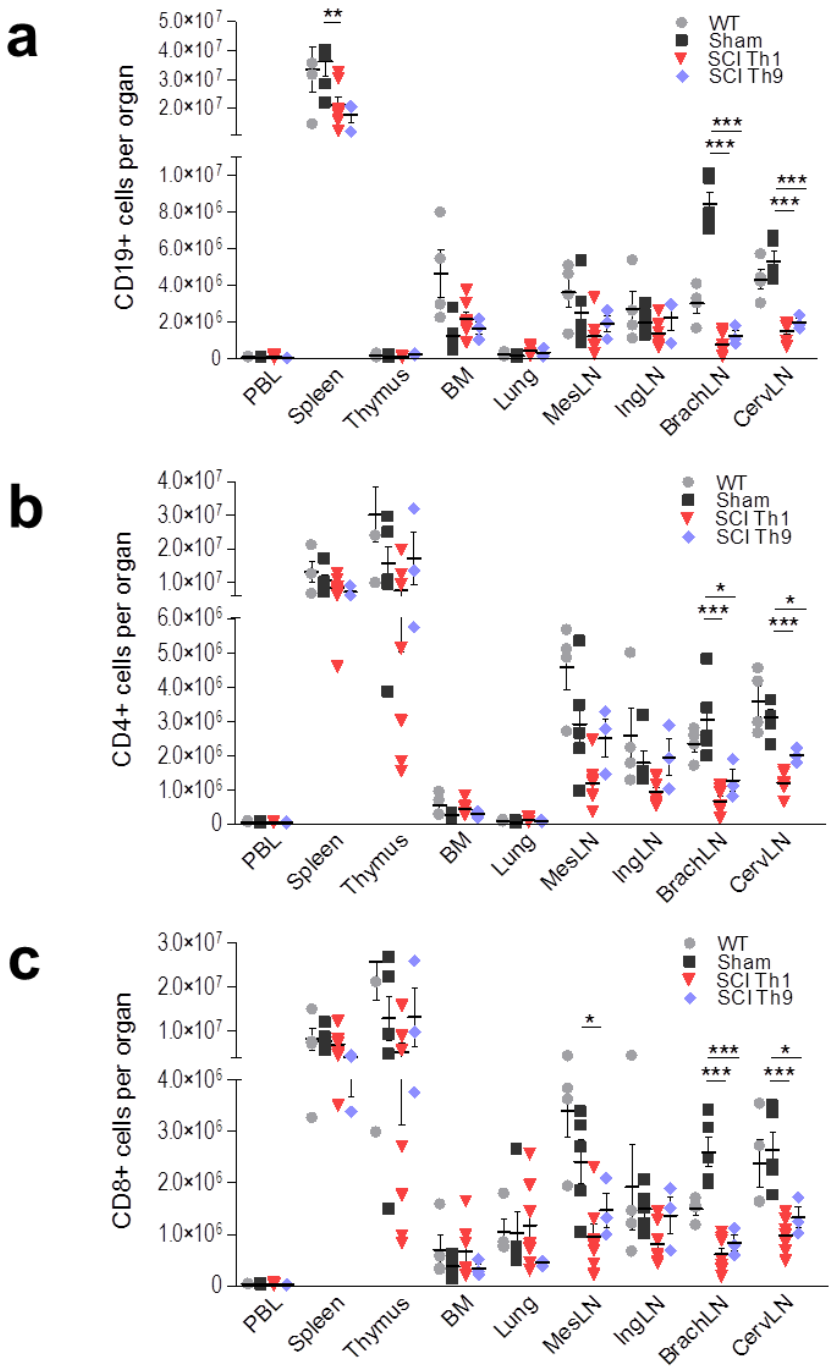

Supplementary Figure 6

Adrenotransplantation reduced effects of lesion height and protected from pneumonia after SCI.

Disconnection of the adrenal glands from spinal innervation (adrenotransplantation) resulted in only subtle differences in organ shrinkage between high versus low thoracic level SCI (Th1/Th9). This held true for all examined cell populations, including $CD4^+$ (**a**), $CD19^+$ (**b**), $CD8^+$ (**c**), $CD11c^+$, and $CD11b^+$ cells (not shown). Data are mean ± SEM, n=3-7 animals per group. * p<0.05; ** p<0.01; *** p<0.001, 1-way ANOVA with Tukey's multiple comparison test.

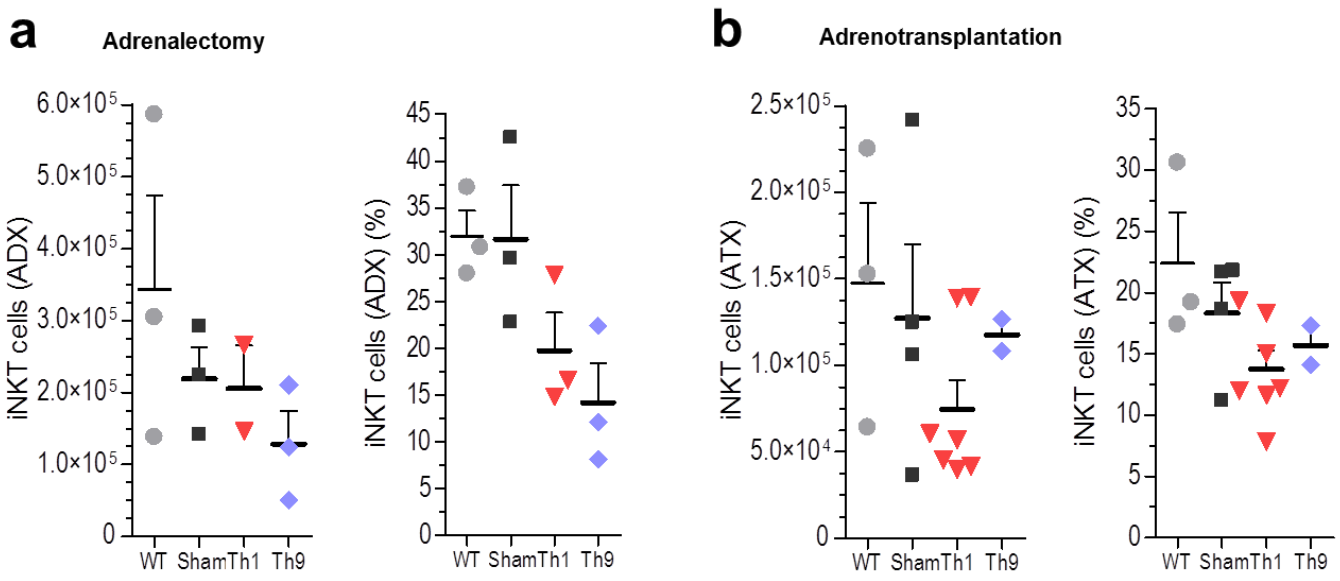

Supplementary Figure 7

The phenotype of liver iNKT cells did not change after SCI.

Numbers and percentages of liver iNKT cells were not altered after experimental SCI in wild-type mice after adrenalectomy (**a**) and adrenotransplantation (**b**). Data are mean ± SEM, n=3-4 animals per group. * $p<0.05$; 1-way ANOVA with Tukey's multiple comparison test.

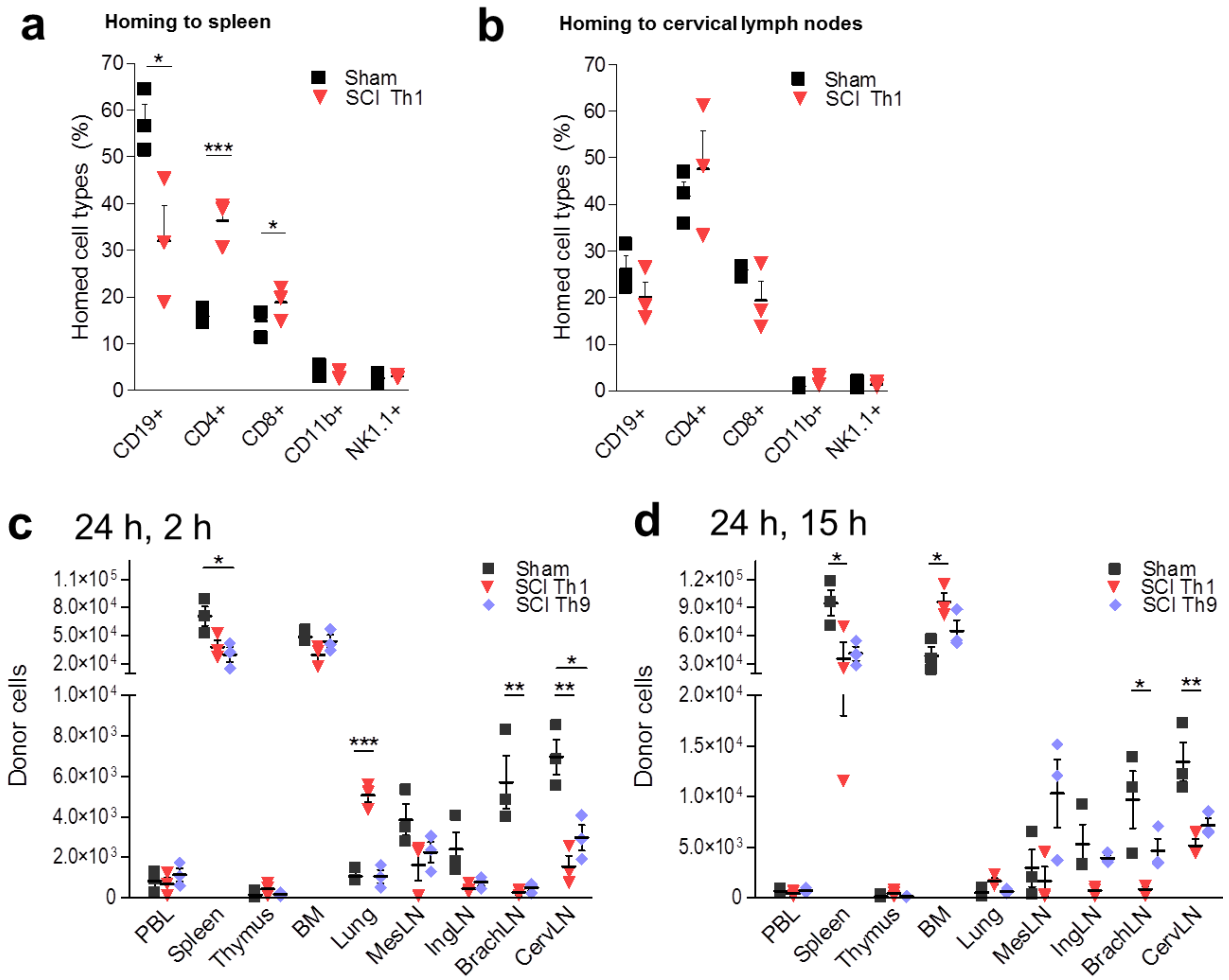

Supplementary Figure 8

Phenotypic characterization of the lymphocyte homing defect.

Homing of injected donor splenocytes (composed of ~52% $CD19^+$, ~23% $CD4^+$, ~17% $CD8^+$ cells) was not equally impaired for all donor cell populations or target organs. (**a**) The homing deficit was most pronounced for B cells with reduced percentage of $CD19^+$ cells (only 30% B cells after SCI compared to almost 60% after sham), while the percentage of T cells in the donor population was increased (despite total reduction). (**b**) In contrast, homing of donor cells to the cervical LNs was equally impaired for all cell populations after SCI. (**c**) The 2-hour homing deficit of donor cells to most organs was detectable already 1 d post SCI, most pronounced to peripheral LNs. (**d**) Not only homing, but also redistribution of donor cells (15 hours cell migration) was severely disturbed after SCI. Data are mean ± SEM, n=3-5 (**a-b**) or 3 (**c-d**) animals per group. * $p<0.05$; ** $p<0.01$; *** $p<0.001$, unpaired Student's t test (**a-b**) or 1-way ANOVA with Tukey's multiple comparison test (**c-d**).

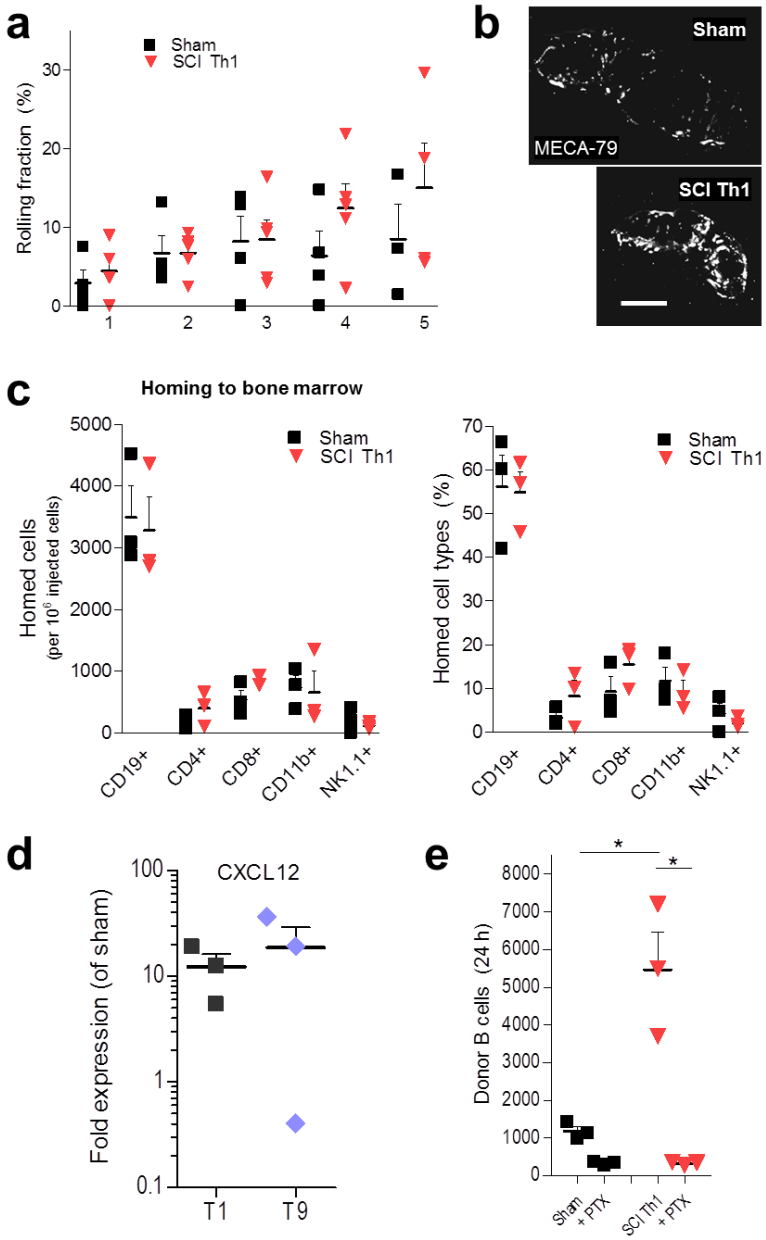

Supplementary Figure 9

Homing behavior of T cells after SCI.

(**a**) *In vivo* imaging of the inguinal LN showed that rolling of T lymphocytes after SCI was not impaired. (**b**) In the shrunken brachial LN after SCI, the expression level of PNAd (MECA-79 antibody) appeared increased. (**c**) In contrast to spleen and LNs, homing to the bone marrow is only slightly changed with a subtle increase of $CD4^+$ and $CD8^+$ T cells. (**d**) BM mRNA expression of CXCL12 was increased. (**e**) BM of injured mice (3d post SCI) recruits ~5 times more mature B cells from the circulation 24 hours after injection. Homing to BM is completely abolished if B cells were pre-treated with pertussis toxin in vitro. Data are mean ± SEM, n=3-5 animals per group. * $p<0.05$; ** $p<0.01$; *** $p<0.001$, unpaired Student's t test. Bar represents 1 mm in **b**.

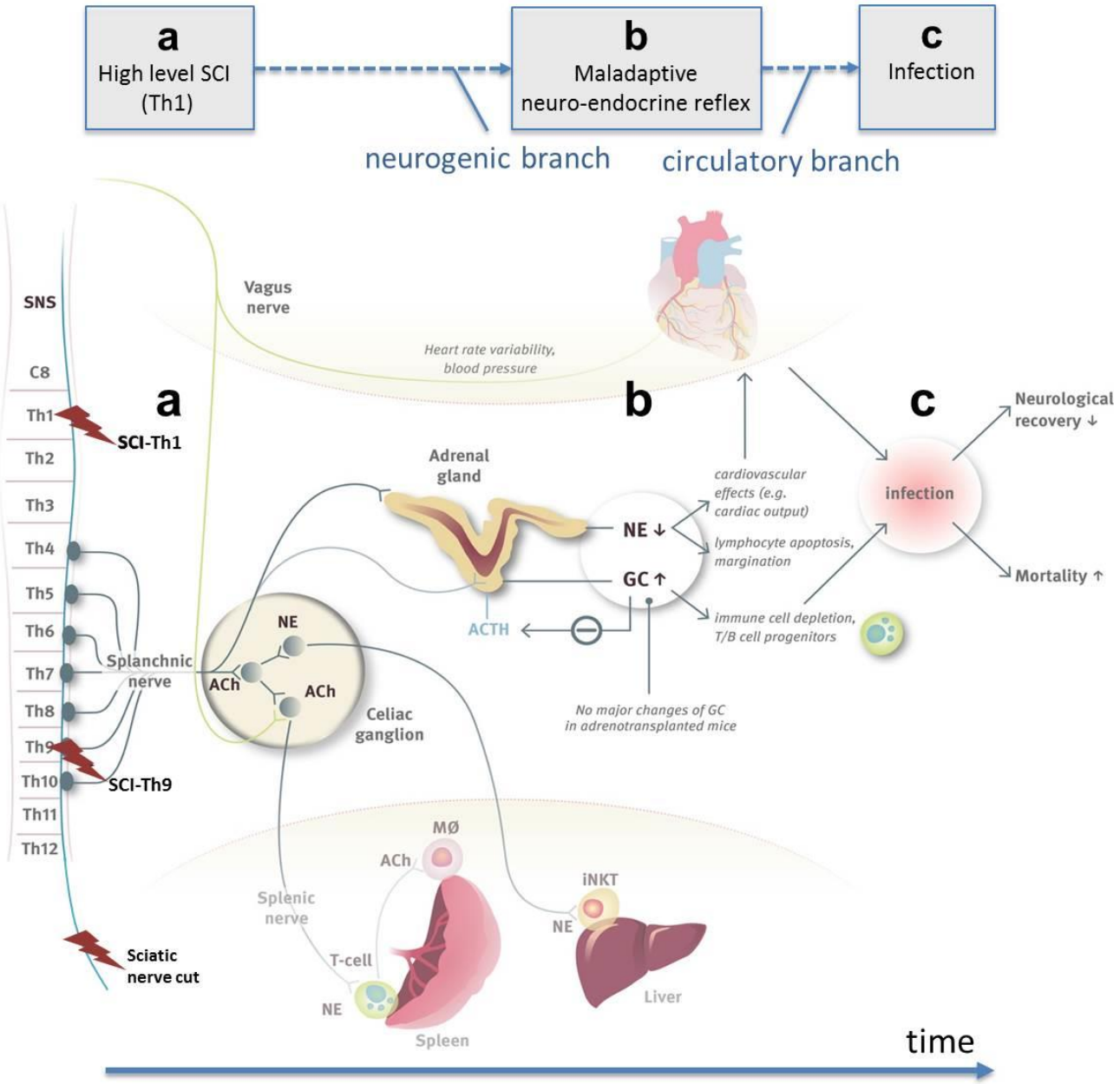

Supplementary Figure 10

Cascade of events showing how SCI ultimately results in neuroendocrine dysfunction involving the adrenal glands and leading to infection.

(**a**) High-level (Th1) SCI interrupts neural vegetative innervation of the adrenal glands from the spinal cord via splanchnic and adrenal nerves. (**b**) Adrenal denervation results in a drop of CA release and in disinhibition of GC release. Increased GCs then suppress ACTH production (primary hypercortisolism). Dysfunctional neuro-endocrine signaling leads to high GC and low NE levels which promote infections via pathways including reduced cardiac output, disturbed lymphocyte trafficking, or increased immune cell apoptosis. (**c**) The susceptibility to pneumonia was reversed if GC levels remained balanced in adrenotransplanted animals. The figure additionally shows how further pathways of immune dysfunction after SCI interfere with the here presented cascade. For example, vagus nerve-mediated parasympathetic innervation of the cardiovascular system (top) or spleen and liver (bottom) intersect with the sympathetic route. This might be of particular relevance to lesions of the central nervous system, which are located above the originating vagus fibers in the brainstem, such as in stroke.